

# SCIENTIFIC REPORTS

OPEN

## Increased GABA<sub>B</sub> receptor signaling in a rat model for schizophrenia

Martijn M. Selten<sup>1,\*</sup>, Francisca Meyer<sup>2,\*</sup>, Wei Ba<sup>1,3</sup>, Astrid Vallès<sup>2,4</sup>, Dorien A. Maas<sup>1,2</sup>, Moritz Negwer<sup>5</sup>, Vivian D. Eijsink<sup>2</sup>, Ruben W. M. van Vugt<sup>2</sup>, Josephus A. van Hulten<sup>2</sup>, Nick H. M. van Bakel<sup>2</sup>, Joey Roosen<sup>2</sup>, Robert J. van der Linden<sup>2</sup>, Dirk Schubert<sup>1</sup>, Michel M. M. Verheij<sup>1</sup>, Nael Nadif Kasri<sup>1,3,†</sup> & Gerard J. M. Martens<sup>2,†</sup>

Received: 11 November 2015

Accepted: 05 September 2016

Published: 30 September 2016

Schizophrenia is a complex disorder that affects cognitive function and has been linked, both in patients and animal models, to dysfunction of the GABAergic system. However, the pathophysiological consequences of this dysfunction are not well understood. Here, we examined the GABAergic system in an animal model displaying schizophrenia-relevant features, the apomorphine-susceptible (APO-SUS) rat and its phenotypic counterpart, the apomorphine-unsusceptible (APO-UNSUS) rat at postnatal day 20–22. We found changes in the expression of the GABA-synthesizing enzyme GAD67 specifically in the prelimbic- but not the infralimbic region of the medial prefrontal cortex (mPFC), indicative of reduced inhibitory function in this region in APO-SUS rats. While we did not observe changes in basal synaptic transmission onto LII/III pyramidal cells in the mPFC of APO-SUS compared to APO-UNSUS rats, we report reduced paired-pulse ratios at longer inter-stimulus intervals. The GABA<sub>B</sub> receptor antagonist CGP 55845 abolished this reduction, indicating that the decreased paired-pulse ratio was caused by increased GABA<sub>B</sub> signaling. Consistently, we find an increased expression of the GABA<sub>B1</sub> receptor subunit in APO-SUS rats. Our data provide physiological evidence for increased presynaptic GABA<sub>B</sub> signaling in the mPFC of APO-SUS rats, further supporting an important role for the GABAergic system in the pathophysiology of schizophrenia.

Schizophrenia is a complex mental disorder thought to result from a combination of genetic and environmental factors that provide vulnerability to early- and later-life stressors<sup>1–3</sup>. Growing evidence suggests that schizophrenia may arise from abnormal connectivity between various integrative brain regions, especially the prefrontal cortex (PFC), the medial temporal lobe, and striatal regions<sup>4–7</sup>. For several decades, schizophrenia research was guided by the dopamine hypothesis<sup>8</sup>. However, this hypothesis has expanded more recently into a view including other neurotransmitters such as serotonin<sup>9</sup>, glutamate<sup>10</sup> and  $\gamma$ -aminobutyric acid (GABA)<sup>11</sup>.

Dysfunction of the GABAergic system in schizophrenia has been well documented by postmortem studies showing alterations in a number of pre- and post-synaptic markers of inhibitory neurotransmission thought to be most prominent in parvalbumin positive (PV<sup>+</sup>) neurons<sup>12</sup>. For example, reduced densities of calbindin-positive (CB<sup>+</sup>) and PV<sup>+</sup> GABAergic interneurons have been observed in the PFC of schizophrenia patients<sup>13–15</sup>. In addition, protein levels of GABA transporter 1 (GAT1) are reduced in the PFC of schizophrenia patients<sup>16</sup>. Also, PFC levels of the GABA synthesizing enzyme GAD67 are reduced in schizophrenia, which can be attributed to reduced expression in PV<sup>+</sup> cells specifically<sup>17</sup> and is indicative of reduced GABAergic signaling<sup>18</sup>. At the synaptic level, the GABAA $\alpha$ 2 subunit, which is prominently expressed in synapses formed by chandelier cells on the axon initial segment of pyramidal neurons, is upregulated in schizophrenia patients<sup>19</sup>. In line with these results, a genetic model of schizophrenia, the Erbb4 knock-out mouse, shows changes in GABAA $\alpha$ 2 and GAT1 density as

<sup>1</sup>Department of Cognitive Neuroscience, Radboud University Medical Center, Donders Institute for Brain, Cognition, and Behaviour, Nijmegen, the Netherlands. <sup>2</sup>Department of Molecular Animal Physiology, Donders Institute for Brain, Cognition and Behaviour, Centre for Neuroscience, Radboud University, Nijmegen, the Netherlands. <sup>3</sup>Department of Human Genetics, Radboud University Medical Center, Donders Institute for Brain, Cognition and Behaviour, Nijmegen, the Netherlands. <sup>4</sup>Department of Cognitive Neuroscience, Faculty of Psychology and Neurosciences, Maastricht University, Maastricht, the Netherlands. <sup>5</sup>Department of Language and Genetics, Max Planck Institute for Psycholinguistics, Nijmegen, the Netherlands. <sup>\*</sup>These authors contributed equally to this work. <sup>†</sup>These authors jointly supervised this work. Correspondence and requests for materials should be addressed to G.J.M.M. (email: G.Martens@ncmls.ru.nl)

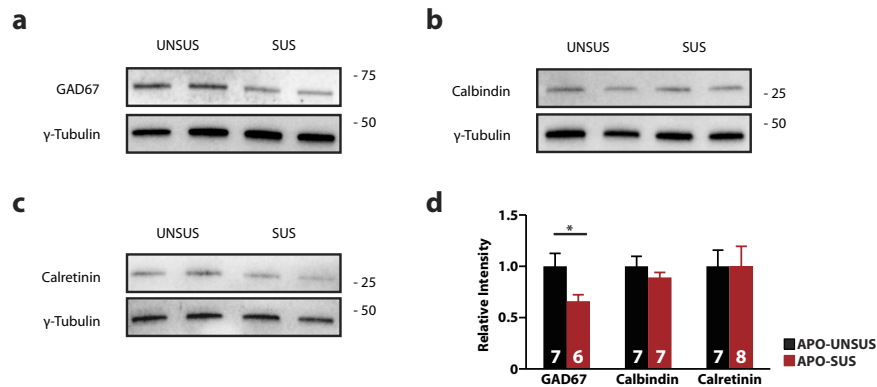


**Figure 1. Reduced expression of GAD67, but not Calbindin (CB) and Calretinin (CR) in the medial prefrontal cortex (mPFC) of APO-SUS rats.** (a–c) Representative immunoblot images for GAD67 (a), CB (b) and CR (c,d) quantification of western blot analysis for CB, CR and GAD67 in APO-UNSUS and APO-SUS mPFC. Expression is normalized to APO-UNSUS expression of the respective protein. Sample size (n) is indicated in the bars. Data is presented as mean  $\pm$  SEM, \*  $p < 0.05$ . Student's t-test.

well as a reduced number of inhibitory synapses on excitatory pyramidal cells<sup>12,20</sup>. Conversely, excitatory inputs onto PV<sup>+</sup> cells are decreased in these mice<sup>12,20</sup>.

To explore the pathophysiological mechanisms underlying schizophrenia, we used the apomorphine-susceptible (APO-SUS) rat model and its phenotypic counterpart, the apomorphine-unsusceptible (APO-UNSUS) rat. These two rat lines have been pharmacogenetically selected and bred from an outbred Wistar population based on their stereotypical gnawing responses to the dopamine D1/D2 agonist apomorphine<sup>21</sup>. The APO-SUS rat is a well-characterized animal model that displays schizophrenia-relevant features during adulthood, such as altered density of central dopamine receptors<sup>22</sup>, high sensitivity to dopaminergic drugs (i.e., apomorphine and amphetamine)<sup>21,23,24</sup>, decreased prepulse inhibition and diminished latent inhibition<sup>24,25</sup>, increased novelty-induced exploration and accumbal dopamine response<sup>21,23,26</sup>, and an increased HPA-axis response to stress<sup>22</sup>, as well as learning and memory deficits<sup>27,28</sup>. However, the pathophysiology underlying the phenotypes observed in this model remains unknown.

In the present study, we compared the inhibitory system in the medial PFC (mPFC) of APO-SUS and APO-UNSUS rats at postnatal day (PND) 20–22. We found a decrease in the protein level of GAD67 as well as a reduced cell-count for GAD67<sup>+</sup> cells specifically in the prelimbic region (PRL) of the mPFC. While basal synaptic transmission onto LII/III pyramidal cells was not different between the two rat lines, we report a decrease in the paired-pulse ratio in APO-SUS rats at longer ( $\geq 150$  ms) intervals compared to APO-UNSUS rats. Importantly, this decrease could be abolished by application of the GABA<sub>B</sub> antagonist CGP 55845, indicating that the decreased paired-pulse ratio was caused by an increased activity in GABA<sub>B</sub> signaling. We indeed observed an increase in GABA<sub>B</sub> receptor expression in the mPFC of APO-SUS rats compared to APO-UNSUS rats. Collectively, our data identify GABA<sub>B</sub> receptor signaling as a possible player in the etiology of schizophrenia.

## Results

**Reduced levels of GAD67 in the mPFC of APO-SUS rats.** Previous studies have reported altered levels of specific interneuron markers in schizophrenia patients<sup>13–17,29</sup>. In order to determine whether the number of GABAergic interneurons is altered in APO-SUS compared to APO-UNSUS rats, we performed western blot analysis to measure the protein expression levels of GAD67, CB and CR in punches from the mPFC of PND 20–22 rats (Fig. 1). We found protein levels of GAD67 to be reduced by  $\sim 35\%$  in APO-SUS rats (Fig. 1a,d;  $p = 0.04$ ). Conversely, we found no change in the levels of CB (Fig. 1b,d;  $p = 0.33$ ) and CR (Fig. 1c,d;  $p = 0.99$ ) between the two rat lines.

**Reduction of GAD67<sup>+</sup> cells in the prelimbic region, but not the infralimbic region, of the mPFC of APO-SUS rats.** Next, we wanted to assess whether the decrease in GAD67 protein levels in the mPFC was due to a decreased amount of GAD67 per cell or to a decrease in the total number of interneurons. To this end we performed immunohistochemistry to assess the number of interneurons positive for GAD67. We also assessed the number of CB<sup>+</sup>, CR<sup>+</sup> and PV<sup>+</sup> cells, which together label  $\sim 90\%$  of GABAergic interneurons<sup>30</sup>. We used coronal sections of the mPFC and analyzed the number of positive cells separately for the prelimbic (PRL)- and infralimbic (IL) region, two subregions of the mPFC.

We found a significant decrease of GAD67<sup>+</sup> cells specifically in the PRL (APO-UNSUS  $6.12 \pm 0.25$  cells/mm<sup>2</sup>; APO-SUS  $5.25 \pm 0.15$  cells/mm<sup>2</sup>,  $p = 0.012$ ; Fig. 2a,b,i), but not the IL (APO-UNSUS  $7.25 \pm 0.29$  cells/mm<sup>2</sup>; APO-SUS  $6.60 \pm 0.28$  cells/mm<sup>2</sup>,  $p = 0.13$ ; Fig. 2a,b,j) in APO-SUS rats. We found no changes in the levels of CB<sup>+</sup>, CR<sup>+</sup> and PV<sup>+</sup> cells in both the PRL (CB<sup>+</sup>: APO-UNSUS  $9.32 \pm 0.79$  cells/mm<sup>2</sup>; APO-SUS  $9.82 \pm 0.60$  cells/mm<sup>2</sup>,  $p = 0.64$ ; CR<sup>+</sup>: APO-UNSUS  $3.06 \pm 0.16$  cells/mm<sup>2</sup>; APO-SUS  $3.43 \pm 0.22$  cells/mm<sup>2</sup>,  $p = 0.19$ ; PV<sup>+</sup>: APO-UNSUS  $2.32 \pm 0.11$  cells/mm<sup>2</sup>; APO-SUS  $2.49 \pm 0.21$  cells/mm<sup>2</sup>,  $p = 0.47$ ), or IL (CB<sup>+</sup>: APO-UNSUS  $10.36 \pm 0.70$  cells/mm<sup>2</sup>; APO-SUS  $9.33 \pm 0.59$  cells/mm<sup>2</sup>,  $p = 0.33$ ; CR<sup>+</sup>: APO-UNSUS

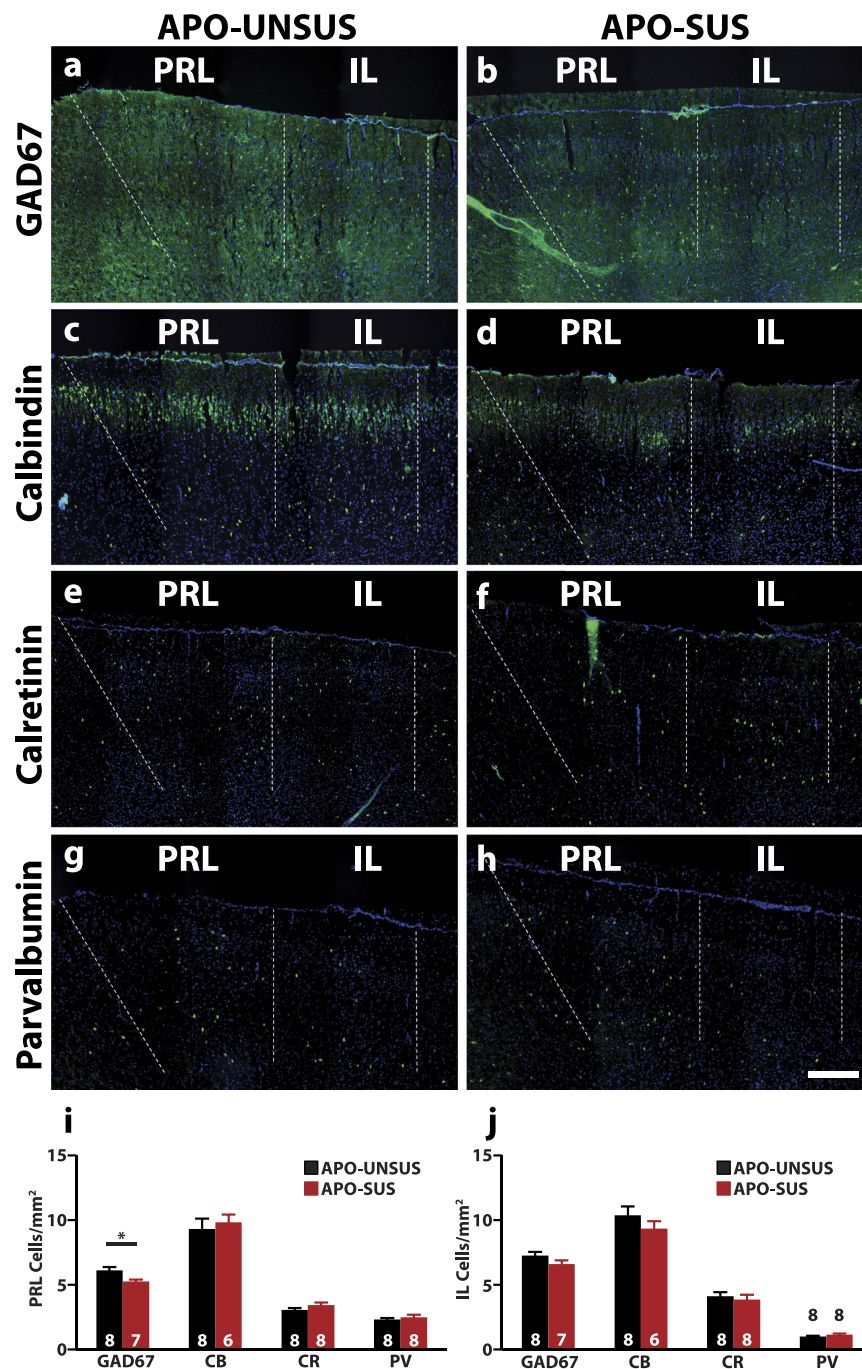


**Figure 2.** Reduced number of GAD67<sup>+</sup> cells in the PRL, but not the IL. Representative images of a staining for GAD67 (a,b), Calbindin (CB) (c,d), Calretinin (CR) (e,f) and parvalbumin (PV) (g,h) and quantification in the prelimbic (PRL) (i) and infralimbic (IL) region (j) of the medial prefrontal cortex. GAD67, CB, CR and PV staining in green, Hoechst in blue. Sample size (n) is indicated in the bars. Scale bar: 200 μm. Data is presented as mean ± SEM. \*\*p < 0.01. Student's t-test.

4.12 ± 0.32 cells/mm<sup>2</sup>; APO-SUS 3.85 ± 0.37 cells/mm<sup>2</sup>, p = 0.58; PV<sup>+</sup>: APO-UNSUS 0.99 ± 0.08 cells/mm<sup>2</sup>; APO-SUS 1.13 ± 0.11 cells/mm<sup>2</sup>, p = 0.30; Fig. 2c–j). The fact that we did not observe changes in the CB<sup>+</sup> CR<sup>+</sup> and PV<sup>+</sup> populations, which suggests the reduction in GAD67 is due to a reduced level of GAD67 per cell, rather than a reduction in the total amount of interneurons, specifically in the PRL.

**Unaltered basal synaptic input on LII/III pyramidal neurons in the mPFC.** Since reduced levels of GAD67 are indicative of reduced interneuronal activity<sup>31,32</sup>, we subsequently tested if the observed changes in GAD67 protein levels would be accompanied by changes at the electrophysiological level. In order to assess basal synaptic input we used whole-cell voltage clamp to record miniature inhibitory postsynaptic currents (mIPSCs)

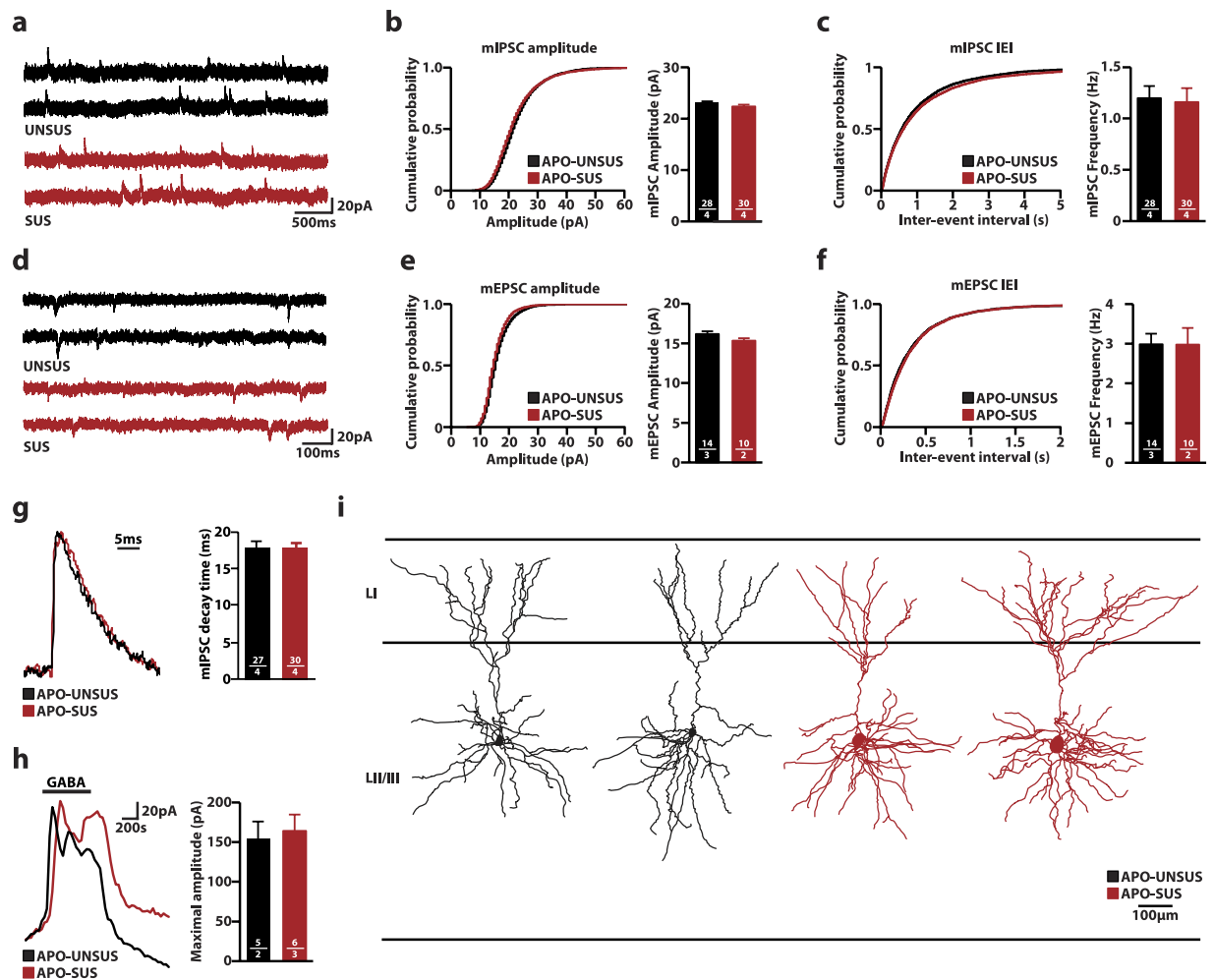


**Figure 3. No changes in basal synaptic transmission and morphology in LII/III pyramidal cells in the medial prefrontal cortex (mPFC).** (a) Representative traces of miniature inhibitory post-synaptic currents (mIPSCs) recorded from LII/III pyramidal cells from acute brain slices from APO-UNSUS and APO-SUS rats. (b,c) Cumulative distributions of mIPSC amplitudes (b) and inter-event intervals (IEI) (c) from APO-UNSUS and APO-SUS rats. (d) Representative traces of miniature excitatory post-synaptic currents (mEPSCs) recorded from LII/III pyramidal cells from acute brain slices from APO-UNSUS and APO-SUS rats (e,f) Cumulative distributions of mEPSC amplitudes (e) and inter-event intervals (f) from APO-UNSUS and APO-SUS rats. (g) Representative traces (scaled) and distribution of mIPSC decay time. (h) Representative traces and quantification of systemic GABA (20  $\mu$ M) application from APO-UNSUS and APO-SUS rats. Black bar indicates GABA application. (i) Representative reconstructions of LII/III pyramidal neurons from mPFC. Sample size (n) is indicated in the bars as number of cells/number of animals. Bar graphs are presented as mean  $\pm$  SEM. Student's t-test.

from layer (L) II/III pyramidal neurons in the mPFC (Fig. 3a–c). We found no difference in both mIPSC amplitude (APO-UNSUS  $23.04 \pm 0.32$  pA; APO-SUS  $22.33 \pm 0.37$  pA,  $p = 0.16$ ) and frequency (APO-UNSUS  $1.20 \pm 0.12$  Hz; APO-SUS  $1.16 \pm 0.14$  Hz,  $p = 0.83$ ). Similarly, no differences were found in miniature excitatory postsynaptic currents (mEPSCs) between the two rat lines (amplitude: APO-UNSUS  $16.20 \pm 0.31$  pA; APO-SUS  $15.34 \pm 0.31$  pA;  $p = 0.08$ ; frequency: APO-UNSUS  $2.99 \pm 0.26$  Hz; APO-SUS  $2.98 \pm 0.42$  Hz,  $p = 0.98$ ) (Fig. 3d–f).

Previous studies have shown that changes in postsynaptic GABA receptor subunit composition are reflected in the decay time of mIPSC<sup>33,34</sup>. We found no changes in the mIPSC decay time in APO-SUS rats (APO-UNSUS  $15.58 \pm 0.52$  ms; APO-SUS  $13.46 \pm 0.93$  ms,  $p = 0.06$ ), indicating the postsynaptic receptor content of inhibitory synapses was unaltered (Fig. 3g).

Next, we measured the maximal response to bath application of 20  $\mu$ M GABA (Fig. 3h). No difference was observed between APO-UNSUS and APO-SUS rats (APO-UNSUS  $154.1 \pm 48.3$  pA; APO-SUS  $163.9 \pm 51.2$  pA,  $p = 0.78$ ), indicating that the total number of GABA<sub>A</sub> receptors was identical. Together, these data show that there is no difference in basal synaptic inhibitory and excitatory input connectivity onto LII/III pyramidal cells in the mPFC between APO-UNSUS and APO-SUS rats.

We then analyzed pyramidal cell morphology of cells that were filled with biocytin during the recordings. All cells had a typical pyramidal morphology, hallmarked by a skirt of basal dendrites radiating  $\sim 200$   $\mu$ m from the

Morphology		UNSUS	SUS	p-value	Sign
Basal Dendrites	Quantity	6.0 ± 0.9	9.3 ± 1.4	0.029	n.s.
	Nodes	18.5 ± 2.1	20.8 ± 2.5	0.404	n.s.
	Ends	24.3 ± 2.6	29.8 ± 1.8	0.060	n.s.
	Length (μm)	2339.9 ± 407.5	2659.7 ± 189.1	0.433	n.s.
	Mean length	397.2 ± 59.1	312.8 ± 54.4	0.224	n.s.
Apical Dendrite	Nodes	15.0 ± 1.7	22.0 ± 4.0	0.093	n.s.
	Ends	16.0 ± 1.7	23.0 ± 4.0	0.093	n.s.
	Length (μm)	1775.9 ± 183.1	2617.7 ± 490.4	0.085	n.s.
	Max Branch Order	8.0 ± 0.5	11.0 ± 0.8	0.009	n.s.
Convex Hull	Area (μm <sup>2</sup> )	43375.2 ± 2899.2	55194.9 ± 8447.3	0.143	n.s.
	Perimeter (μm)	831.0 ± 20.8	929.5 ± 66.6	0.116	n.s.

**Table 1. Dendritic morphological analysis of reconstructed layer II/III pyramidal cells.** Student's t-test with Holm-Sidak correction for multiple comparisons. Data is presented as mean ± SEM. Sign: significance; n.s: not significant.

soma, and a single long apical dendrite that reached into upper LI (Fig. 3i). The apical dendrite mostly branched close to the soma, and had an apical tuft close to the pia mater, mainly within LI, consistent with previous reports<sup>35</sup>. The dendritic morphology of both apical and basal dendrites did not differ between pyramidal cells from APO-UNSUS and APO-SUS rats (Table 1).

#### Reduction in paired-pulse ratio through GABA<sub>B</sub> receptor signaling in the mPFC of APO-SUS rats.

Next, we investigated the release probability of inhibitory synapses onto LII/III pyramidal cells by recording the paired-pulse ratio following stimulation in the same layer in the PFC. We recorded paired-pulse ratios at different inter-stimulus intervals (ISI) (Fig. 4a,b) and found that the paired-pulse ratio were indistinguishable between both rat lines for short ISIs ( $\leq 100$  ms) (50 ms APO-UNSUS  $0.96 \pm 0.03$ ; APO-SUS  $0.94 \pm 0.04$ ,  $p = 0.67$ ; 100 ms APO-UNSUS  $0.92 \pm 0.03$ ; APO-SUS  $0.89 \pm 0.04$ ,  $p = 0.65$ ), whereas LII/III pyramidal cells from APO-SUS rats showed a reduced paired-pulse ratio at longer ISIs ( $\geq 150$  ms) (150 ms APO-UNSUS  $0.88 \pm 0.03$ ; APO-SUS  $0.77 \pm 0.02$ ;  $p < 0.01$ ; 200 ms APO-UNSUS  $0.81 \pm 0.03$ ; APO-SUS  $0.71 \pm 0.02$ ;  $p < 0.01$ ; 500 ms APO-UNSUS  $0.82 \pm 0.02$ ; APO-SUS  $0.75 \pm 0.02$ ;  $p < 0.05$ ; Fig. 4b). Whereas changes at short ISIs are indicative of an altered release probability, changes in paired-pulse ratios for longer ISIs can be indicative of reduced presynaptic calcium inflow<sup>36</sup>. Previous studies have shown that a reduced presynaptic calcium inflow can be caused by increased retrograde signaling via nitric oxide<sup>37</sup> and endocannabinoids<sup>38</sup>, or through binding of GABA to presynaptic GABA<sub>B</sub> receptors, which upon activation negatively influence Ca<sup>2+</sup> inflow through voltage gated Ca<sup>2+</sup>-channels<sup>39</sup>. Since only GABA<sub>B</sub> receptors act at the sub-second time range, we investigated the involvement of GABA<sub>B</sub> receptor signaling by recording the paired-pulse ratio in the presence of the GABA<sub>B</sub> receptor antagonist CGP 55845. In APO-SUS rats, the paired-pulse ratio at 50 ms and 100 ms was unaffected by CGP 55845, consistent with GABA<sub>B</sub> receptor activation time<sup>40</sup>. Interestingly, we found that the reduced paired-pulse ratio at longer ISIs (150, 200 and 500 ms) was completely abolished in the presence of CGP 55845 (50 ms APO-UNSUS  $0.90 \pm 0.03$ ; APO-SUS  $0.89 \pm 0.05$ ,  $p = 0.75$ ; 100 ms APO-UNSUS  $0.88 \pm 0.02$ ; APO-SUS  $0.84 \pm 0.02$ ,  $p = 0.29$ ; 150 ms APO-UNSUS  $0.81 \pm 0.01$ ; APO-SUS  $0.82 \pm 0.04$ ,  $p = 0.68$ ; 200 ms APO-UNSUS  $0.79 \pm 0.02$ ; APO-SUS  $0.82 \pm 0.03$ ,  $p = 0.38$ ; 500 ms APO-UNSUS  $0.81 \pm 0.02$ ; APO-SUS  $0.83 \pm 0.02$ ,  $p = 0.24$ ; Fig. 4c,d), indicating that increased GABA<sub>B</sub> receptor signaling underlies the decreased paired-pulse ratio in APO-SUS compared to APO-UNSUS rats. Of note, blocking of GABA<sub>B</sub> receptors with CGP 55845 had no effect on the paired-pulse ratio of APO-UNSUS rats at all ISIs tested (Fig. 4e,f), indicating that GABA<sub>B</sub> receptor signaling does not play a role in these experiments in APO-UNSUS rats.

#### Increased expression of GABA<sub>B</sub> receptors, but not GAT1, in the mPFC of APO-SUS rats.

The increase in GABA<sub>B</sub> receptor signaling could be caused either by an increase of GABA<sub>B</sub> receptor activation, through increased levels of extracellular GABA, or by an increase in the number of GABA<sub>B</sub> receptors. Increased levels of extracellular GABA could be caused by a reduction in the expression of GAT1, the main GABA transporter in the central nervous system<sup>41</sup>. GAT1 reduces the amount of extracellular GABA in the synapse, which reduces spillover<sup>41</sup>. GABA<sub>B</sub> receptors are located perisynaptically, and are activated by GABA spillover. In addition, reduced GAT1 expression has been found in schizophrenia patients<sup>42</sup> and animal models<sup>12</sup> of schizophrenia. We therefore first assessed the levels of GAT1 in punches from the mPFC of APO-SUS and APO-UNSUS rats by performing western blot analysis. However, we found no significant difference between APO-SUS and APO-UNSUS rats ( $p = 0.73$ ; Fig. 5a,b). We next studied the protein expression levels of GABA<sub>B</sub> receptors. Western blot analysis using an antibody against the GABA<sub>B1</sub> subunit, which together with the GABA<sub>B2</sub> receptor forms an active GABA<sub>B</sub> receptor<sup>43</sup>, revealed that the levels of GABA<sub>B1</sub> were increased by ~110% in the mPFC of APO-SUS rats compared to APO-UNSUS mPFC ( $p < 0.05$ ; Fig. 5a,b). Together, our data suggest that increased GABA<sub>B</sub> receptor signaling in APO-SUS rats is accompanied by increased expression of the GABA<sub>B1</sub> subunit, and underlies the decreased paired-pulse ratio in APO-SUS rats.

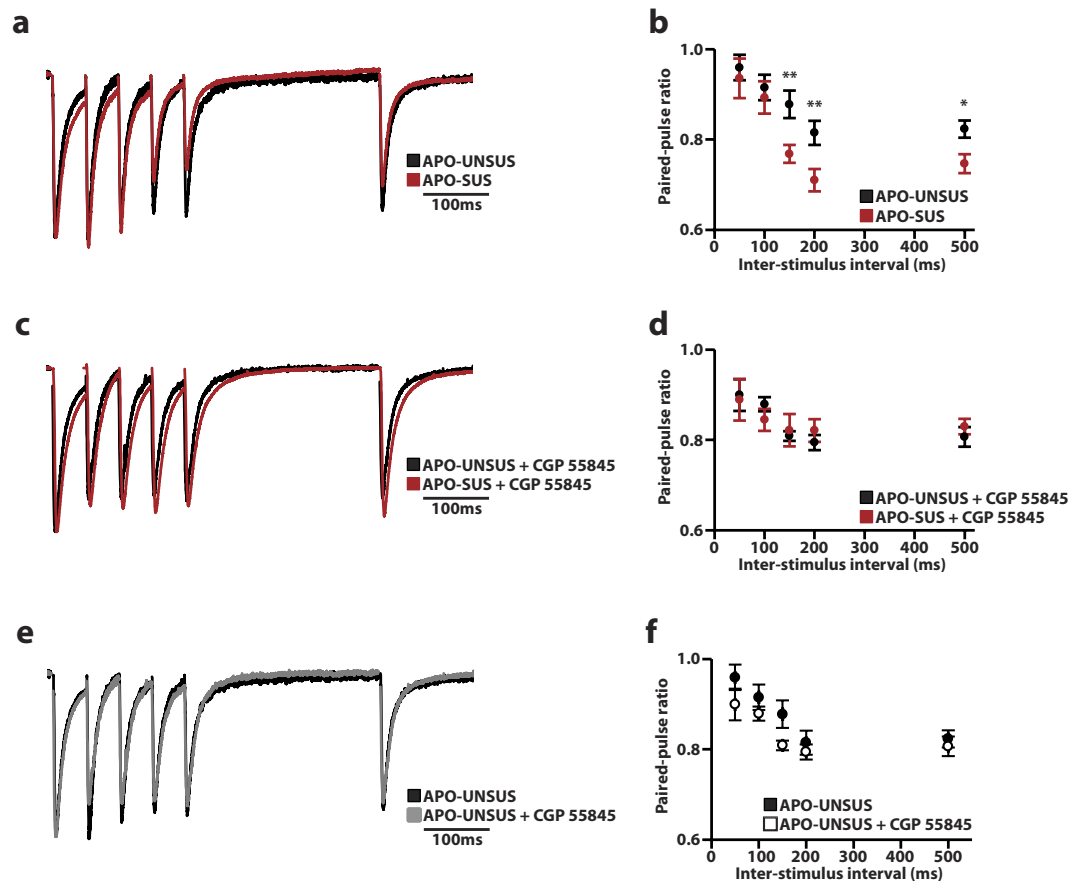


**Figure 4.** APO-SUS rats show a reduced paired-pulse ratio at long  $\geq 150$  ms inter-stimulus intervals (ISI). (a,b) Representative traces (a) and quantification (b) of the paired-pulse ratio at different ISIs from APO-UNSUS ( $n = 14/3$ ) and APO-SUS ( $n = 15/4$ ) rats. (c,d) Representative traces (c) and quantification (d) of the paired-pulse ratio at different ISIs in the presence of the GABA<sub>B</sub> antagonist CGP 55845 from APO-UNSUS ( $n = 10/3$ ) and APO-SUS ( $n = 12/3$ ) rats. (e,f) Comparison between APO-UNSUS in the absence or presence of CGP 55845, note that these traces are the same as in a–d. Representative traces show an overlay of all 5 individual inter-stimulus intervals. Sample size ( $n$ ) is shown as number of cells/number of animals. Data are presented as mean  $\pm$  SEM. \* $p < 0.05$ ; \*\* $p < 0.01$ . Student's t-test with Holm-Sidak correction for multiple comparisons.

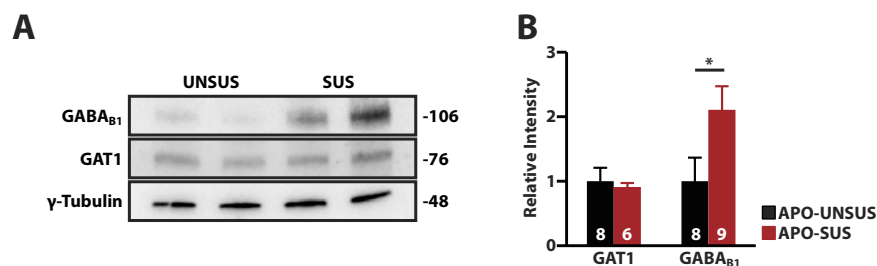


**Figure 5.** The expression of GABA<sub>B1</sub>, but not GAT1, is increased in the medial prefrontal cortex of APO-SUS rats. (a) Representative blot and (b) quantification of western blot analysis for GAT1 and GABA<sub>B1</sub> on APO-UNSUS and APO-SUS. Expression is normalized to APO-UNSUS expression of the respective protein. Sample size ( $n$ ) is indicated in the bars. Data is presented as mean  $\pm$  SEM, \* $p < 0.05$ . Student's t-test.

## Discussion

The GABAergic system plays an important role in the pathophysiology of schizophrenia<sup>44,45</sup>. Here, using the APO-SUS/APO-UNSUS rat model at PND 20–22 we further highlight the importance of dysfunctional GABA signaling in schizophrenia-related traits. We provide several lines of evidence for deficits in the inhibitory

circuitry within the PRL of APO-SUS rats: (i) a reduced level of GAD67 in interneurons in the mPFC of APO-SUS rats, specifically in the PRL; (ii) a reduced paired-pulse ratio at longer ( $\geq 150$  ms) ISIs in APO-SUS rats; and (iii) increased GABA<sub>B</sub> signaling due to an increased expression of the GABA<sub>B1</sub> subunit of the GABA<sub>B</sub> receptor. Finally, we were able to reverse the increased GABA<sub>B</sub> signaling in APO-SUS rats by the application of the GABA<sub>B</sub> antagonist CGP 55845.

In our present study on the GABAergic system in the APO-SUS rats, we observed a decreased protein level of GAD67 in the PRL. Also, we found a reduced number of GAD67<sup>+</sup> cells in this region. However, the number of CB<sup>+</sup>, CR<sup>+</sup> and PV<sup>+</sup> neurons, which together account for ~90% of interneurons<sup>30</sup>, remained unchanged in the APO-SUS rat, indicating that the total number of interneurons is unaltered. The reduced number of GAD67<sup>+</sup> cells could result from a reduction of GAD67 levels per cell, causing these interneurons to be under the detection threshold of our analysis. Indeed, reduced levels of GAD67 have been reported before in schizophrenia both in animal models and post-mortem patient studies<sup>17,46,47</sup>.

A number of studies has shown that reduced prefrontal inhibitory transmission induces various cognitive, emotional and dopaminergic abnormalities that resemble aspects of schizophrenia<sup>48</sup>. More specifically, reduced GABAergic activity in the PRL of the rat PFC results in deficits in speed of processing information, cognitive flexibility, recall of relevant information and enhanced dopamine activity<sup>49,50</sup>. In this respect, it is of interest to note that GABAergic interneurons in the mPFC receive direct input from mesocortical dopaminergic fibers, and this control matures during adolescence and appears crucial for cortical network activity at adulthood<sup>51</sup>. Moreover, together with the genetic background and environmental stress the developmental ingrowth of dopaminergic fibers may lead to an abnormal functioning of the GABAergic interneurons at adulthood, especially under stressful conditions that also alter the dopamine system<sup>52</sup>. A functional dysregulation of the mesostriatal dopaminergic neurons in schizophrenia has indeed been well established<sup>8,53,54</sup>.

Given that we found altered levels of GAD67 in the mPFC of APO-SUS rats, indicative of a reduced inhibitory drive, we studied changes in the basal synaptic input connectivity of LII/III pyramidal neurons. Surprisingly, mIPSC amplitude and frequency on these neurons were unaltered, as was the presynaptic release probability for GABA, suggesting that the changes in interneuron composition were not accompanied by changes in basal synaptic input. Additionally, we did not observe any changes in the response to bath application of GABA, indicating that the total number of GABA<sub>A</sub> receptors was unaltered. Together, these results suggest that the total number and strength of inhibitory synapses are not different between APO-SUS and APO-UNUSUS rats. However, this study does not include a measure of excitability of the individual classes of interneurons within the mPFC and it is conceivable that the reduced inhibitory activity is due to a reduced excitability of one or more subclasses of interneurons. The use of reporter rodent lines will allow the targeted exploration of the excitability of specific interneuron subclasses in future studies.

While we did not observe differences at the level of synaptic transmission and morphology of LII/III pyramidal cells, we found a clear reduction in the paired-pulse ratio in the APO-SUS compared to APO-UNUSUS rats. This reduction was specific for ISIs  $\geq 150$  ms, and was not observed in  $\leq 100$  ms ISIs. The reduced paired-pulse ratio at  $\geq 150$  ms ISIs indicates a reduced release of neurotransmitter at the second pulse. We show that enhanced GABA<sub>B</sub> receptor signaling, at least in part, underlies this reduction. Indeed, the paired-pulse ratio in the APO-SUS rats could be restored to the levels observed in the APO-UNUSUS rats by application of the GABA<sub>B</sub> receptor antagonist CGP 55845. GABA<sub>B</sub> receptors are metabotropic G-protein-coupled GABA receptors, and are located perisynaptically at both the pre- and postsynapse<sup>55</sup>. Presynaptic GABA<sub>B</sub> receptors reduce calcium inflow mainly by inhibiting N-type and P/Q type voltage-gated calcium channels and to a lesser extent by activating inward-rectifying potassium channels such as Kir3, causing a hyperpolarization<sup>55</sup>. Both pathways reduce the inflow of calcium, and occur with a delay of ~150 ms and slow decay of ~1 s<sup>40</sup> consistent with the maximal effect that we observed at the 150 ms ISI. Postsynaptic GABA<sub>B</sub> receptors mediate opening of potassium channels, but both the absence of an outward current in our recordings as well as the use of a cesium-based intracellular recording solution exclude the possibility of a postsynaptic contribution of GABA<sub>B</sub> receptors to our recordings and point to presynaptic GABA<sub>B</sub> receptor activity underlying the observed changes. Activation of presynaptic GABA<sub>B</sub> receptors reduces calcium conductance and subsequent GABA release, and therefore provides a negative feedback to the GABAergic system<sup>56,57</sup>. Interestingly, a reduced inhibitory input onto excitatory pyramidal cells has been found in models for schizophrenia<sup>20</sup> and autism<sup>58</sup>, and underlines the notion that a proper tuning of excitation and inhibition is required for proper brain function<sup>11</sup>. Importantly, a number of studies have highlighted a crucial link between GABA transmission and cognitive dysfunction in schizophrenia, indicating that reduced prefrontal inhibitory transmission induces various cognitive, emotional and dopaminergic abnormalities that resemble aspects of this disorder<sup>48</sup>.

Consistent with our finding of increased GABA<sub>B</sub> signaling, we show that the expression of GABA<sub>B1</sub> is increased in the mPFC of APO-SUS compared to APO-UNUSUS rats. However, our results do not show if the increase in GABA<sub>B1</sub> is due to an increase in the number of GABA<sub>B1</sub>-expressing cells, or an increase in the amount of GABA<sub>B1</sub> per cell. Thus far, no comparative studies are available describing the levels of GABA<sub>B</sub> receptors in individual interneuron subtypes. Interestingly, a reduction in GABA<sub>B</sub> subunit expression has been observed in various brain regions of schizophrenia patients<sup>59–61</sup>. In humans, stimulation of cortical GABA<sub>B</sub> receptors in the fronto-parietal network has led to better attentional allocation in reinforcement learning<sup>62</sup>. In addition, GABA<sub>B</sub> receptor manipulation has been shown to reverse behavioral changes related to psychosis<sup>63</sup>, improve pre-pulse inhibition deficits and ameliorate sensorimotor gating in rodent models<sup>64</sup>. Combining the results of the present animal study with the results of the previously reported patient studies suggests that both reduced as well as increased GABA<sub>B</sub> signaling may underlie some of the aspects of schizophrenia. Of note, most schizophrenia research on patients is hampered by the use of medication, whereas the rat model used in this study is drug naive. Additional preclinical studies are warranted to further evaluate the hypothesis that the GABA<sub>B</sub> receptor

represents a promising pharmacological target for treating appropriately stratified subsets of individuals with schizophrenia.

It is important to notice that schizophrenia is a disorder with an onset during adolescence or early adulthood<sup>65</sup>. The PND 20–22 rats used for this study are in their early adolescence, and therefore do not necessarily display the schizophrenia-relevant features that have been described in adult rats<sup>21–26</sup>. Even though the exact mechanisms underlying neurodevelopmental disorders, including schizophrenia, are unknown, many theories exist about a distorted balance between neuronal excitation and inhibition during development<sup>51,66,67</sup>. While it is difficult to distinguish primary effects from homeostatic- and compensatory mechanisms, a substantial amount of evidence points in the direction of disrupted inhibitory signaling as an important factor in the etiology of schizophrenia<sup>51,68,69</sup>. Our data suggest a possible role for GABA<sub>B</sub> receptor signaling in the development of the schizophrenia-relevant features observed in adult APO-SUS rats.

In conclusion, our findings highlight the importance of GABAergic signaling for inducing schizophrenia-related phenotypes, and identify GABA<sub>B</sub> receptors as potential new key players in the distorted network functioning in this disorder.

## Methods

**Animals.** All experiments were performed with male Wistar (PND20–22) rats pharmacogenetically selected for high susceptibility (APO-SUS) or low susceptibility (APO-UNSUS) to apomorphine. The generation of APO-SUS and APO-UNSUS rat lines has been described previously<sup>21</sup>. In short, upon injection of apomorphine, a bimodal distribution of the gnawing response was found, i.e. approximately 40% of the Wistar rats showed a weak gnawing response (<10 counts/45 min) and a similar percentage showed an intense gnawing response (>500 counts/45 min). Following this initial selection, the nine males and females with the highest scores, and the nine males and females with the lowest scores were paired and their offspring was again tested for their gnawing response. For each new generation, nine new pairs of rats were selected out of the four male and female litters showing the highest (APO-SUS) and the lowest (APO-UNSUS) mean gnawing response per gender, with the condition that brother/sister pairing was not allowed. APO-SUS rats are defined as animals born from an APO-SUS mother and father; APO-UNSUS rats are likewise defined as animals born from an APO-UNSUS mother and father. The present experiments were performed with naive male APO-SUS and APO-UNSUS rats belonging to the 38<sup>th</sup> and 40<sup>th</sup> generation, i.e. apomorphine was used only during the procedure to select and generate the APO-SUS and APO-UNSUS lines.

All rats were bred and reared in the Central Animal Facility of the Radboud University Nijmegen. The animals were reared and housed in macrolon cages (42 × 26 × 15 cm) in a controlled (20 ± 2 °C) and enriched environment under a 12 h light/dark cycle (lights on at 7:00 A.M.). Food pellets and water were provided ad libitum. Experimental procedures were performed between 9:00 A.M. and 5:00 P.M. The experimental procedures were approved by the Animal Ethics Committee of the Radboud University Nijmegen (Nijmegen, the Netherlands) and conducted in accordance with the Dutch legislation. Every effort was made to minimize the number of animals used and their suffering.

**Western blotting.** For the western blot experiments the animals were decapitated and the brains were collected quickly, frozen on dry ice, and kept at –80 °C. The brains were sliced into 200 μm coronal sections using a cryostat (Microm HM 500OM) at –15 °C and mounted on glass slides. Punches from 6 sections of the mPFC (prelimbic and infralimbic region) were taken with a 2 mm diameter micropunch needle (Harris Inc.) between the first appearance of the corpus callosum and the start of the caudate putamen. The coordinates were determined according to the atlas of Paxinos and Watson<sup>70</sup>. Samples from each hemisphere were pooled. All the samples were stored at –80 °C before protein extraction took place.

Brain punches were homogenized in 50 μl of lysis buffer (50 mM Hepes pH 7.4, 140 mM NaCl, 0.1% Triton-X100, 1% Tween 20, 0.1% deoxycholate) supplemented with protease inhibitor mix (Roche Diagnostics). The protein levels were assessed using the Bradford assay. After protein measurement, sodium dodecyl sulfate polyacrylamide gel electrophoresis (SDS-PAGE) on 10% (w/v) at 100 V for 90 minutes was carried out using a Mini-Protean system (Bio-Rad, USA). Protein (40 μg) was loaded in each lane with loading buffer (0.25 M Tris-HCl, pH 6.8, 2% SDS, 10% glycerol, 0.25% bromophenolblue, 4% beta-mercaptoethanol). After electrophoresis, proteins were transferred to a polyvinylidene fluoride membrane (PVDF, Amersham, Hybond-P), using an electrophoretic transfer system (Bio-Rad, USA) at 400 mA for 90 minutes. The membranes were then blocked with 5% skimmed milk dissolved in 0.1 M PBS for one hour. The membranes were incubated overnight at 4 °C with the primary antibodies diluted in blocking buffer containing 5% skimmed milk dissolved in a PBS Tween 20 mixture (5%) (PBS-T, Sigma-Aldrich). The primary antibodies were the following: mouse monoclonal antibodies for CB D-28K (1:1000, Swant), CR (1:1000, Swant), GAD67 (1:1000, Abcam), GAT1 (1:500, Abcam), GABAB1 (1:500, Abcam), and gamma-tubulin (1:10000, Sigma). After being washed for one hour with 1% skimmed milk in PBS-T (0.05%), the membranes were incubated for one hour in the dark at room temperature with goat-anti-mouse secondary antibody (1:10,000; LI-COR Biosciences Inc; IRDye 680). The membranes were imaged using an Odyssey IR-scanner (LI-COR Biosciences, Inc.) and the generated pictures were quantified using the Odyssey software (LI-COR Biosciences Inc.). The levels of protein expression were normalized to beta-tubulin. Protein expression values are normalized to APO-UNSUS values (relative intensity).

**Immunohistochemistry.** For the fluorescent immunohistochemistry experiments, rats were sacrificed by direct decapitation without anesthesia, after which the brains were extracted and post-fixed by immersion in 2% paraformaldehyde (PFA) in 0.1 M PBS, pH 7.4 for 48 hours. After post-fixation, the brains were transferred to a 30% sucrose solution for cryoprotection. Coronal sections (10 μm) were cut on cryostat, collected on SuperFrost glass slides and stored at –20 °C until further processing.



Sections (10  $\mu\text{m}$ ) were incubated for 1 h in blocking buffer (5% normal goat, horse and donkey serum, 1% BSA, 1% glycine, 0.1% lysine, 0.4% Triton X-100) to minimize nonspecific labeling. Tissue sections were then incubated overnight at room temperature with mouse monoclonal primary antibodies diluted in blocking buffer against CB D-28k (1:2000; CB300; Swant), CR (1:3500; CR-6B3, Swant), or PV (1:8000; PV-235, Swant); for GAD67 (1:5000; K-87, Abcam), incubation was done for 4 h at room temperature, followed by a 65 h incubation at 4 °C. The next morning, sections were washed in PBS and placed for 1.5 h in a 1:500 dilution of goat-anti-mouse Alexa-fluor 488 secondary antibody (Invitrogen). Hoechst (bisBenzimide dye, No 33342, Sigma B-2261; 1  $\mu\text{g}/\text{mL}$  prepared in 0.1 M PBS) staining was performed for nuclear staining. After overnight drying of the sections at room temperature, they were coverslipped with FluorSave™ Reagent (Merck Millipore). The next day, slides were visualized with an automated high content epifluorescence microscope with digital image acquisition (Leica DMI6000B inverted microscope, Leica EL6000 illumination source). The pictures were manually analyzed and quantified at 10X magnification using FIJI3 in a blinded fashion. The values obtained for each animal represent the average of measurements taken from 3–4 equally spaced sections for each brain area. Nomenclature of the brain was based on the atlas of Paxinos and Watson<sup>70</sup>.

**Electrophysiology.** Rats were anesthetized with isoflurane before decapitation. Coronal slices (350  $\mu\text{m}$ ) were cut using a HM650V vibration microtome (Thermo Scientific) in ice cold artificial cerebrospinal fluid (ACSF) containing (in mM): 124 NaCl; 11 Glucose; 3 KCl; 1.25  $\text{NaH}_2\text{PO}_4$ ; 1  $\text{CaCl}_2$ ; 4  $\text{MgCl}_2$ ; 26  $\text{NaHCO}_3$ , continuously oxygenated with 95%  $\text{O}_2$ /5%  $\text{CO}_2$  and incubated for 1 h at room temperature. Slices were transferred to the recording setup 15 minutes prior to recording and incubated at 30 °C while being continuously oxygenated with 95%  $\text{O}_2$ /5%  $\text{CO}_2$  in recording ACSF containing (unless otherwise stated) (in mM): 124 NaCl, 1.25  $\text{NaH}_2\text{PO}_4$ , 3 KCl, 26  $\text{NaHCO}_3$ , 10 Glucose, 2  $\text{CaCl}_2$ , 1  $\text{MgCl}_2$ . Patch pipettes (3–5 M $\Omega$ ) were made from borosilicate glass capillaries and filled with intracellular solution containing (in mM): 115 CsMeSO<sub>3</sub>; 20 CsCl; 10 HEPES; 2.5  $\text{MgCl}_2$ ; 4  $\text{Na}_2\text{ATP}$ ; 0.4  $\text{NaGTP}$ ; 10 Na-Phosphocreatine; 0.6 EGTA. Traces were recorded using a Multiclamp 700B amplifier (Molecular Devices), sampled at 10 kHz and filtered at 2 kHz. Cells were excluded from analysis if the series resistance exceeded 25 M $\Omega$ . mIPSCs were recorded in the presence of Tetrodotoxin (TTX, 1  $\mu\text{M}$ ), 6-cyano-7-nitroquinoxaline-2,3-dione (CNQX, 5  $\mu\text{M}$ ) and (2R)-amino-5-phosphonovaleric acid (APV, 100  $\mu\text{M}$ ) at a holding potential of +10 mV. mEPSC were recorded in the presence of TTX and Picrotoxin (PTX, 100  $\mu\text{M}$ ) at a holding potential of –60 mV. Paired-pulse ratio (PPR) was recorded following stimulation in LII/III of the PFC in the presence of CNQX and D-APV, in ACSF containing 4 mM  $\text{CaCl}_2$  and 4 mM  $\text{MgCl}_2$  to increase the stimulated responses, at a holding potential of –60 mV. Stimulation strength was set to evoke a ~200 pA response to the first stimulus. Two 1 ms pulses were given with a 50 ms, 100 ms, 150 ms, 200 ms or 500 ms interval. PPR was calculated as peak2/peak1 after correcting for any residual current at the second pulse. CGP 55845 was used at a concentration of 10  $\mu\text{M}$ <sup>71</sup>. For GABA application, cells were allowed to stabilize their holding current, after which 20  $\mu\text{M}$  GABA was washed in. We quantified the maximal change in holding current as the maximal response to the washed in GABA. Miniature recordings were analyzed using Mini Analysis Program (Synaptosoft). Other traces were analyzed using Clampfit 10.2. All drugs were purchased from Tocris.

**Morphological reconstructions.** For morphological reconstructions, the internal solution was supplemented with 0.4% biocytin (Sigma-Aldrich). Following single-cell electrophysiology, the slices with biocytin-filled neurons were fixated in 4% paraformaldehyde in 0.1 M PBS overnight at 4 °C, and subsequently processed following a modified staining protocol based on Marx *et al.*<sup>72</sup>. In brief: after fixation, slices were rinsed in 0.1 M PB, incubated in 3%  $\text{H}_2\text{O}_2$  in 0.1 M PB for 30 minutes at room temperature to quench endogenous peroxidases, rinsed in 0.1 M PBS, then incubated in Avidin-Biotin-Peroxidase solution (Vectastain Elite, with 1% v/v Triton-100) overnight on a shaking platform at 4 °C. The next day, slices were washed with 0.1 M PBS and pre-incubated with Di-Aminobenzidine (DAB) solution with Nickel enhancer (Vector Peroxidase substrate kit, SK-4100) for 30 min. Then, the DAB solution was replaced with the same solution plus  $\text{H}_2\text{O}_2$  and incubated for ca. 30 seconds. Slices were then rinsed in 0.1 M PB, mounted on gelatinized coverslips, and dried for 3–6 h in a custom-made moist chamber at room temperature. Slices were dehydrated in an ethanol series and Xylene, put on coverslips and sealed with Eukitt (Sigma). Slices were imaged on a Zeiss Axioskop 1 upright brightfield microscope with 20x and 40x objectives (Zeiss EC Plan-Neofluar, NA 0.5 and 0.75, respectively) and motorized stage (MicroBrightField). The camera and motorized stage were connected to a NeuroLucida workstation (MicroBrightField). Cells were selected based on position in the cortical layer II/III of the prefrontal cortex, pyramidal morphology, and staining intensity. Somata, apical and basal dendrites were reconstructed in NeuroLucida as three-dimensional drawings. Reconstructions were analysed in NeuroExplorer (MicroBrightField) for intrinsic parameters and Sholl analysis.

**Statistical analysis.** Statistical analysis was performed using Prism (Graphpad). Significance was tested with a two-sided Student's t-test. Correction for multiple comparisons was performed using the Holm-Sidak method where indicated. Data is expressed as mean  $\pm$  SEM. Significance was defined as  $p < 0.05$  (\*) or  $p < 0.01$  (\*\*).

## References

- Sullivan, P. F., Kendler, K. S. & Neale, M. C. Schizophrenia as a Complex Trait. *Arch. Gen. Psychiatry* **60**, 1187–1192 (2003).
- Tsuang, M. T., Bar, J. L., Stone, W. S. & Faraone, S. V. Gene-environment interactions in mental disorders. *World Psychiatry* **3**, 73–83 (2004).
- Burrows, E. L. & Hannan, A. J. Decanalization mediating gene-environment interactions in schizophrenia and other psychiatric disorders with neurodevelopmental etiology. *Front. Behav. Neurosci.* **7**, 1–5 (2013).
- Lawrie, S. M. *et al.* Reduced frontotemporal functional connectivity in schizophrenia associated with auditory hallucinations. *Biol. Psychiatry* **51**, 1008–1011 (2002).
- Stephan, K. E., Friston, K. J. & Frith, C. D. Dysconnection in Schizophrenia: From abnormal synaptic plasticity to failures of self-monitoring. *Schizophr. Bull.* **35**, 509–527 (2009).

6. Meyer-Lindenberg, A. From maps to mechanisms through neuroimaging of schizophrenia. *Nature* **468**, 194–202 (2010).
7. Fornito, A., Yoon, J., Zalesky, A., Bullmore, E. T. & Carter, C. S. General and specific functional connectivity disturbances in first-episode schizophrenia during cognitive control performance. *Biol. Psychiatry* **70**, 64–72 (2011).
8. Kuepper, R., Skinbjerg, M. & Abi-Dargham, A. In *Current Antipsychotics* 1–26 (2012).
9. Bhattacharyya, S., Raote, L., Bhattacharya, A., Mileli, R. & Panicker, M. M. Activation, internalization, and recycling of the serotonin 2A receptor by dopamine. *Proc. Natl. Acad. Sci. USA* **103**, 15248–15253 (2006).
10. Moghaddam, B. & Javitt, D. From Revolution to Evolution: The Glutamate Hypothesis of Schizophrenia and its Implication for Treatment. *Neuropsychopharmacology* **37**, 4–15 (2012).
11. Marin, O. Interneuron dysfunction in psychiatric disorders. *Nat. Rev. Neurosci.* 107–120, doi: 10.1038/nrn3155 (2012).
12. Del Pino, I. *et al.* Erbb4 deletion from fast-spiking interneurons causes schizophrenia-like phenotypes. *Neuron* **79**, 1152–1168 (2013).
13. Beasley, C. L., Zhang, Z. J., Patten, I. & Reynolds, G. P. Selective deficits in prefrontal cortical GABAergic neurons in schizophrenia defined by the presence of calcium-binding proteins. *Biol. Psychiatry* **52**, 708–715 (2002).
14. Reynolds, G. P., Abdul-Monim, Z., Reynolds, G. P., Zuhali Neill, J. C. & Zhang, Z. Calcium Binding Protein Markers of GABA Deficits in Schizophrenia - Post Mortem Studies and Animal Models. *Neurotox. Res.* **6**, 57–61 (2004).
15. Sakai, T. *et al.* Changes in density of calcium-binding-protein-immunoreactive GABAergic neurons in prefrontal cortex in schizophrenia and bipolar disorder. *Neuropathology* **28**, 143–150 (2008).
16. Schleimer, S. B., Hinton, T., Dixon, G. & Johnston, G. A. R. GABA transporters GAT-1 and GAT-3 in the human dorsolateral prefrontal cortex in schizophrenia. *Neuropsychobiology* **50**, 226–230 (2004).
17. Hashimoto, T. *et al.* Gene expression deficits in a subclass of GABA neurons in the prefrontal cortex of subjects with schizophrenia. *J. Neurosci.* **23**, 6315–6326 (2003).
18. Lazarus, M. S., Krishnan, K. & Huang, Z. J. GAD67 Deficiency in Parvalbumin Interneurons Produces Deficits in Inhibitory Transmission and Network Disinhibition in Mouse Prefrontal Cortex. *Cereb. Cortex* 1290–1296, doi: 10.1093/cercor/bht322 (2013).
19. Volk, D. W. *et al.* Reciprocal alterations in pre- and postsynaptic inhibitory markers at chandelier cell inputs to pyramidal neurons in schizophrenia. *Cereb. Cortex* **12**, 1063–1070 (2002).
20. Fazzari, P. *et al.* Control of cortical GABA circuitry development by Nrg1 and ErbB4 signalling. *Nature* **464**, 1376–1380 (2010).
21. Cools, A. R., Brachten, R., Heeren, D., Willems, A. & Ellenbroek, B. Search after neurobiological profile of individual-specific features of Wistar rats. *Brain Res. Bull.* **24**, 49–69 (1990).
22. Rots, N. Y. *et al.* Rats bred for enhanced apomorphine susceptibility have elevated tyrosine hydroxylase mRNA and dopamine D2-receptor binding sites in nigrostriatal and tuberoinfundibular dopamine systems. *Brain Res.* **710**, 189–196 (1996).
23. Cools, A. R., Ellenbroek, B. A., Gingras, M. A., Engbersen, A. & Heeren, D. Differences in vulnerability and susceptibility to dexamphetamine in Nijmegen high and low responders to novelty: A dose-effect analysis of spatio-temporal programming of behaviour. *Psychopharmacology (Berl.)* **132**, 181–187 (1997).
24. Van der Elst, M. C. J., Ellenbroek, B. A. & Cools, A. R. Cocaine strongly reduces prepulse inhibition in apomorphine-susceptible rats, but not in apomorphine-unsusceptible rats: Regulation by dopamine D2 receptors. *Behav. Brain Res.* **175**, 392–398 (2006).
25. Ellenbroek, B. A., Geyer, M. A. & Cools, A. R. The behavior of APO-SUS rats in animal models with construct validity for schizophrenia. *J. Neurosci.* **15**, 7604–7611 (1995).
26. Van Der Elst, M. C. J. *et al.* A single exposure to novelty differentially affects the accumbal dopaminergic system of apomorphine-susceptible and apomorphine-unsusceptible rats. *Life Sci.* **76**, 1391–1406 (2005).
27. Cools, A. R. *et al.* Apomorphine-susceptible and apomorphine-unsusceptible Wistar rats differ in novelty-induced changes in hippocampal dynorphin B expression and two-way active avoidance: A new key in the search for the role of the hippocampal-accumbens axis. *Behav. Brain Res.* **55**, 213–221 (1993).
28. Tuinstra, T. *et al.* Retrieval of spatial information in Nijmegen high and low responders: involvement of beta-adrenergic mechanisms in the nucleus accumbens. *Behav. Neurosci.* **114**, 1088–1095 (2000).
29. Daviss, S. R. & Lewis, D. A. Local circuit neurons of the prefrontal cortex in schizophrenia: selective increase in the density of calbindin-immunoreactive neurons. *Psychiatry Res.* **59**, 81–96 (1995).
30. Lund, J. S. & Lewis, D. A. Local circuit neurons of developing and mature macaque prefrontal cortex: Golgi and immunocytochemical characteristics. *J. Comp. Neurol.* **328**, 282–312 (1993).
31. Lau, C. G. & Murthy, V. N. Activity-dependent regulation of inhibition via GAD67. *J. Neurosci.* **32**, 8521–8531 (2012).
32. Jiao, Y., Zhang, C., Yanagawa, Y. & Sun, Q.-Q. Major Effects of Sensory Experiences on the Neocortical Inhibitory Circuits. *J. Neurosci.* **26**, 8691–8701 (2006).
33. Okada, M., Onodera, K., Van Renterghem, C., Sieghart, W. & Takahashi, T. Functional correlation of GABA(A) receptor alpha subunits expression with the properties of IPSCs in the developing thalamus. *J. Neurosci.* **20**, 2202–2208 (2000).
34. Dunning, D. D., Hoover, C. L., Soltesz, I., Smith, M. A. & Dowd, D. K. O. GABA A Receptor – Mediated Miniature Postsynaptic Currents and  $\alpha$ -Subunit Expression in Developing Cortical Neurons. *J. Neurophysiol.* 3286–3297 (2014).
35. Van Aerde, K. I. & Feldmeyer, D. Morphological and Physiological Characterization of Pyramidal Neuron Subtypes in Rat Medial Prefrontal Cortex. *Cereb. Cortex* 788–805, doi: 10.1093/cercor/bht278 (2013).
36. Caillard, O., McLean, H. A., Ben-ari, Y. & Gaïarsa, J. Ontogenesis of Presynaptic GABA(B) Receptor-Mediated Inhibition in the CA3 Region of the Rat *Hippocampus* 1341–1348 (1998).
37. Volgushev, M., Balaban, P., Chistiakova, M. & Eysel, U. T. Retrograde signalling with nitric oxide at neocortical synapses. *Eur. J. Neurosci.* **12**, 4255–4267 (2000).
38. Wilson, R. I. & Nicoll, R. A. Endogenous cannabinoids mediate retrograde signalling at hippocampal synapses. *Nature* **410**, 2–6 (2001).
39. Olpe, H.-R., Steinmann, M. W., Greiner, K. & Pozza, M. F. Contribution of presynaptic GABA-B receptors to paired-pulse depression of GABA-responses in the hippocampus. 473–477 (1994).
40. Chalifoux, J. R. & Carter, A. G. GABA B Receptor Modulation of Voltage-Sensitive Calcium Channels in Spines and Dendrites. **31**, 4221–4232 (2011).
41. Gonzalez-Burgos, G., Rotaru, D. C., Zaitsev, A. V., Povysheva, N. V. & Lewis, D. A. GABA transporter GAT1 prevents spillover at proximal and distal GABA synapses onto primate prefrontal cortex neurons. *J. Neurophysiol.* **101**, 533–547 (2009).
42. Volk, D. W., Austin, M. C., Pierri, J. N., Sampson, A. R. & Lewis, D. A. GABA transporter-1 mRNA in the prefrontal cortex in schizophrenia: Decreased expression in a subset of neurons. *Am. J. Psychiatry* **158**, 256–265 (2001).
43. Jones, K. *et al.* GABA(B) receptors function as a heteromeric assembly of the subunits GABA(B)R1 and GABA(B)R2. *Nature* **396**, 674–679 (1998).
44. Nakazawa, K. *et al.* GABAergic interneuron origin of schizophrenia pathophysiology. *Neuropharmacology* **62**, 1574–1583 (2012).
45. Pocklington, A. J. *et al.* Novel Findings from CNVs Implicate Inhibitory and Excitatory Signaling Complexes in Schizophrenia. *Neuron* **86**, 1203–1214 (2015).
46. Guidotti, A. *et al.* Decrease in Reelin and Glutamic Acid Decarboxylase 67 (GAD 67) Expression in Schizophrenia and Bipolar Disorder. *Arch. Gen. Psychiatry* **57**, 1061–1069 (2000).
47. Akbarian, S. & Huang, H. S. Molecular and cellular mechanisms of altered GAD1/GAD67 expression in schizophrenia and related disorders. *Brain Res. Rev.* **52**, 293–304 (2006).

48. Tse, M. T., Piantadosi, P. T. & Floresco, S. B. Prefrontal Cortical Gamma-Aminobutyric Acid Transmission and Cognitive Function: Drawing Links to Schizophrenia from Preclinical Research. *Biol. Psychiatry* **77**, 929–939 (2015).
49. Enomoto, T., Tse, M. T. & Floresco, S. B. Reducing prefrontal gamma-aminobutyric acid activity induces cognitive, behavioral, and dopaminergic abnormalities that resemble schizophrenia. *Biol. Psychiatry* **69**, 432–441 (2011).
50. Piantadosi, P. T. & Floresco, S. B. Prefrontal cortical GABA transmission modulates discrimination and latent inhibition of conditioned fear: Relevance for schizophrenia. *Neuropsychopharmacology* **39**, 2473–2484 (2014).
51. O'Donnell, P. Adolescent onset of cortical disinhibition in schizophrenia: Insights from animal models. *Schizophr. Bull.* **37**, 484–492 (2011).
52. Benes, F. M. & Berretta, S. GABAergic interneurons: implications for understanding schizophrenia and bipolar disorder. *Neuropsychopharmacology* **25**, 1–27 (2001).
53. Laruelle, M., Frankle, W. G., Narendran, R., Kegeles, L. S. & Abi-Dargham, A. Mechanism of action of antipsychotic drugs: From dopamine D2 receptor antagonism to glutamate NMDA facilitation. *Clin. Ther.* **27** (2005).
54. Carlsson, A. *et al.* Interactions Between Monoamines, Glutamate, and GABA in Schizophrenia: New Evidence. *Annu. Rev. Pharmacol. Toxicol.* **63**, 108–116 (2001).
55. Benarroch, E. E. GABAB receptors: structure, functions, and clinical implications. *Neurology* **78**, 578–584 (2012).
56. Davies, C. H., Starkey, S. J., Pozza, M. F. & Collingridge, G. L. GABAB autoreceptors regulate the induction of LTP. *Nature* **349**, 609–611 (1991).
57. Leung, L. S. & Peloquin, P. GABAB receptors inhibit backpropagating dendritic spikes in hippocampal CA1 pyramidal cells *in vivo*. *Hippocampus* **16**, 388–407 (2006).
58. Gibson, J. R., Huber, K. M. & Südhof, T. C. Neuroligin-2 deletion selectively decreases inhibitory synaptic transmission originating from fast-spiking but not from somatostatin-positive interneurons. *J. Neurosci.* **29**, 13883–13897 (2009).
59. Mizukami, K. *et al.* Immunohistochemical localization of gamma-aminobutyric acid(B) receptor in the hippocampus of subjects with schizophrenia. *Neurosci. Lett.* **283**, 101–104 (2000).
60. Mizukami, K. *et al.* Immunohistochemical localization of GABA B receptor in the entorhinal cortex and inferior temporal cortex of schizophrenic brain. *Prog. Neuropsychopharmacol. Biol. Psychiatry* **26**, 393–396 (2002).
61. Fatemi, S. H., Folsom, T. D. & Thuras, P. D. Deficits in GABAB receptor system in schizophrenia and mood disorders: A postmortem study. *Schizophr. Res.* **128**, 37–43 (2011).
62. Ort, A., Kometer, M., Rohde, J., Seifritz, E. & Vollenweider, F. X. The role of GABAB receptors in human reinforcement learning. *Eur. Neuropsychopharmacol.* **24**, 1606–1614 (2014).
63. Wierońska, J. M. *et al.* The GABA B receptor agonist CGP44532 and the positive modulator GS39783 reverse some behavioural changes related to positive syndromes of psychosis in mice. *Br. J. Pharmacol.* **163**, 1034–1047 (2011).
64. Frau, R. *et al.* Positive Allosteric Modulation of GABAB Receptors Ameliorates Sensorimotor Gating in Rodent Models. *CNS Neurosci. Ther.* **20**, 679–684 (2014).
65. Fatemi, S. H. & Folsom, T. D. The neurodevelopmental hypothesis of Schizophrenia, revisited. *Schizophr. Bull.* **35**, 528–548 (2009).
66. Mullins, C., Fishell, G. & Tsien, R. W. Review Unifying Views of Autism Spectrum Disorders : A Consideration of Autoregulatory Feedback Loops. *Neuron* **89**, 1131–1156 (2016).
67. Nelson, S. B. & Valakh, V. Excitatory/Inhibitory Balance and Circuit Homeostasis in Autism Spectrum Disorders. *Neuron* **87**, 684–698 (2015).
68. del Pino, I. *et al.* Erbb4 Deletion from Fast-Spiking Interneurons Causes Schizophrenia-like Phenotypes. *Neuron* **79**, 1152–1168 (2013).
69. Yu, Z. *et al.* GABA Transporter-1 Deficiency Confers Schizophrenia-Like Behavioral Phenotypes. *PLoS One* **8** (2013).
70. Paxinos, G. & Watson, C. *The Rat Brain in Stereotaxic Coordinates* 4th edition (Academic Press, 1998).
71. Deidda, G. *et al.* Reversing excitatory GABAAR signaling restores synaptic plasticity and memory in a mouse model of Down syndrome. *Nat. Med.* **21**, 318–326 (2015).
72. Marx, M., Günter, R. H., Hucko, W., Radnikow, G. & Feldmeyer, D. Improved biocytin labeling and neuronal 3D reconstruction. *Nat. Protoc.* **7**, 394–407 (2012).

## Acknowledgements

The authors thank Jason M. Keller for proofreading the manuscript. The research of the authors was supported by a Hypatia fellowship award of the Radboudumc [to N.N.K.]; EU-FP7 Marie Curie International Reintegration Grant 277091 [to N.N.K.]; the Jerome Lejeune Foundation [to N.N.K.]; Dutch Top Institute Pharma grant T5-209 [to G.J.M.M.].

## Author Contributions

M.M.S., F.M., N.N.K. and G.J.M.M. conceived and designed the experiments; V.D.E. and R.W.M.v.V. assisted in the development of the project; M.M.S., F.M., W.B., A.V., D.A.M., M.N., J.A.v.H., N.H.M.v.B., J.R. and R.J.v.d.L. performed the *in vitro* cell studies, biochemistry studies, and animal experiments; M.M.S., F.M., W.B., A.V., D.A.M., M.N. and M.M.M.V. analyzed and interpreted data under supervision of D.S., N.N.K. and G.J.M.M.; M.M.S. and F.M. wrote the manuscript/prepared the draft of the manuscript; All authors reviewed the manuscript; G.J.M.M. and N.N.K. provided financial support for the project.

## Additional Information

**Competing financial interests:** The authors declare no competing financial interests.

**How to cite this article:** Selten, M. M. *et al.* Increased GABA<sub>B</sub> receptor signaling in a rat model for schizophrenia. *Sci. Rep.* **6**, 34240; doi: 10.1038/srep34240 (2016).



This work is licensed under a Creative Commons Attribution 4.0 International License. The images or other third party material in this article are included in the article's Creative Commons license, unless indicated otherwise in the credit line; if the material is not included under the Creative Commons license, users will need to obtain permission from the license holder to reproduce the material. To view a copy of this license, visit <http://creativecommons.org/licenses/by/4.0/>

© The Author(s) 2016